OPTICAL REVIEW Vol. 21, No. 5 (2014) 698–704

Optical System Design and Experimental Evaluation of a Coherent Doppler Wind Lidar System for the Predictive Control of Wind Turbine

Leilei SHINOHARA[1]*, Julian Asche TAUSCHER[1], Thorsten BEUTH[1], Nico HEUSSNER[2], Maik FOX[1], Harsha Umesh BABU[1], and Wilhelm STORK[1,2]

[1]*Karlsruhe Institute of Technology, Engesserstrasse 5, 76131 Karlsruhe, Germany*
[2]*FZI Forschungszentrum Informatik, Haid und Neu Strasse 10-14, 76131 Karlsruhe, Germany*

(Received March 31, 2014; Revised May 27, 2014; Accepted June 9, 2014)

The control of wind turbine blade pitch systems by Lidar assisted wind speed prediction has been proposed to increase the electric power generation and reduce the mechanical fatigue load on wind turbines. However, the sticking point of such Lidar systems is the price. Hence, our objective is to develop a more cost efficient Lidar system to support the pitch control of horizontal axis wind turbines and therefore to reduce the material requirement, lower the operation and maintenance costs and decrease the cost of wind energy in the long term. Compared to the state of the art Lidar systems, a laser with a shorter coherence length and a corresponding fiber delay line is introduced for reducing the costs. In this paper we present the experimental evaluation of different sending and receiving optics designs for such a system from a free space laboratory setup.

Keywords: optical system design, laser Doppler velocimetry, lidar, atmospheric scattering

1. Introduction

Nowadays large horizontal axis wind turbines (HAWTs) are set up in locations which are difficult to access, e.g., offshore. These locations add an overhead to the production costs as well as the operation and maintenance (O&M) costs. Electricity generation of HAWTs can be improved by a pitch control system which is based on Lidar assisted wind speed prediction.[1,2)] At the International Conference on Optics–Photonics Design & Fabrication (ODF14), we have presented several designs of sending and receiving optics and their evaluations.[3)] In the here presented article, we elaborate further on the details of the optical design for a cost efficient coherent Doppler Lidar (CDL) system for the predictive control of HAWTs that we first introduced as a concept in 2012.[4)] CDL systems have been proven as accurate, reliable sensors for the remote sensing of atmospheric wind velocities since 1966.[5,6)] It works on the principle of measuring the Doppler frequency shift of back scattered light from atmospheric aerosols and molecules for obtaining the wind speed. The Doppler frequency shift δf is proportional to the line-of-sight (LOS) wind speed V [$\delta f = (2V\nu)/c = 2V/\lambda$], with c as the speed of light, ν and λ as the laser frequency and the corresponding wavelength. The CDL concept for HAWTs is depicted in Fig. 1. A measurement system based on this principle was implemented in a wind turbine in April 2010 by the Technical University Denmark (DTU) Risø.[7)]

Nevertheless, the control of wind turbines as a function of wind speed by the Lidar measurement in front of the rotor was already proposed in 1989.[8)] In 2004, the British government establishment QinetiQ has patented a Lidar system for the control of HAWTs, which is located in the hub and directed the beam to the rotation axis of the rotor.[9)] The wind field in front of the rotor is sampled in a cone-shaped form. In a further embodiment they claimed a multiplexed system in a laser beam can be transmitted sequentially over a number of beams in different directions. However the current Lidar system product is in a high price. For example, the ZephIR Lidar is currently priced at ca. €135,000 with the lifetime of about 5 years.[10)] This price is too high for a continuous usage on a HAWT, and thus only pilot projects and wind field measurements are performed during the location determination phase. Therefore, the development of a cost efficient system for HAWT is an attractive proposition. The DTU Risø patented a low cost Lidar system based on a semiconductor laser,[11)] followed by the patent "Multiple directional Lidar system"[12)] from the DTU spin-off Windar Photonics. In this patent, a sensor system consists of an amplified infrared laser based on a 1.5 µm vertical-external cavity surface-emitting laser (VECSEL) with a linewidth of 40 kHz for 2 km coherence

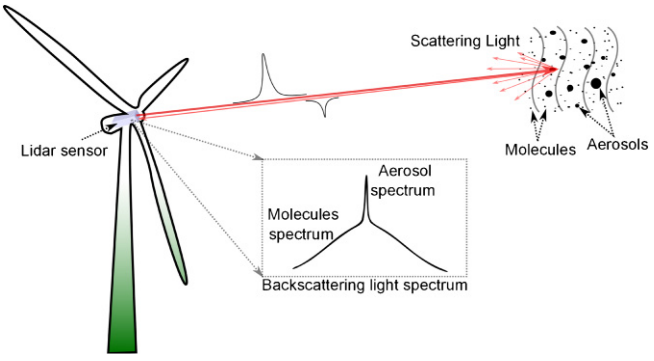

Fig. 1. (Color online) Concept of the coherent Doppler wind Lidar system for the predictive pitch control of HAWT.

*E-mail address: shinohara@kit.edu

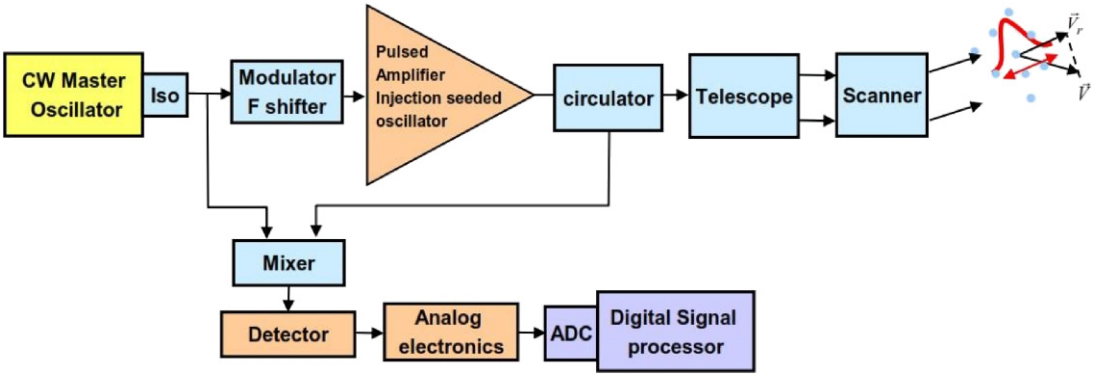

Fig. 2. (Color online) Sketch of a standard pulse Lidar system.[17)]

length and output power in the order of 0.6 W. However, the system can only measure at a fixed distance of 60 m in front of the HAWT which is in the induction zone of the rotor upstream. It is known from the stream tube theory that wind speed changes in this range nonlinearly depending on blade design, pitch angle, tip speed ratio, etc.[13)]

Figure 2 shows a general pulse Lidar system, which contains a (continues wave) CW master oscillator (MO) laser source, a frequency shifter (AOM, acousto-optic modulator/shifter), a pulsed amplifier (EDFA, erbium-doped fiber amplifiers), a circulator, a telescope receiver, a scanner, a mixer (fiber coupler), a detector unit, a signal pre-processing analog electronics unit, an analog to digital converter (ADC) and a digital signal processing (DSP) unit.[17)] The system requires some ten milliwatts optical power laser with a long coherence length of several kilometers. The laser beam is divided into the local oscillator (LO) beam and the MO beam. The MO beam is amplified by a pulsed EDFA to gain a high pulse energy. The circulator is used to transmit the laser to the telescope and direct the back scattering light into the detection unit. Normally, the polarization is used by the circulator to assure a good performance.[18)] The telescope focuses the beam at long distances and collects the backscattering light. A telescope with a larger diameter can transmit the laser pulse with less divergence into a longer distance and collect more signal. A scanner is used to direct the beam into different directions, since the Lidar measures the LOS wind speed only. Therefore, in order to obtain the three dimensional wind vector, measurements from different directions are necessary. The major cost of this system is on the laser and amplifier (ca. €20,000–30,000) and the scanner unit (ca. €10,000). To overcome these cost factors, our concept is based on a 1.5 µm CW semiconductor laser with an erbium-doped fiber amplifier (EDFA) to gain a higher output power. An optical coherent detection method is chosen for measuring the Doppler frequency on the back scattering signal. A comparatively low cost short coherence length laser (ca. €6,000) with a multi-length fiber delay line is used for achieving a multiple distance measurement. The signal to noise ratio (SNR) is usually limited due to the high phase noise and therefore such short coherence length lasers are not used for coherent Doppler Lidar applications. However, by using a fiber delay line to match the initial phase, a laser with a shorter coherence length of several ten meters is found to be sufficient.[14,15)] Furthermore, a fixed receiver and transmitter setup is used to avoid the high price scanner unit as well.

2. System Design and Experimental Validation

For a cost efficient system design, only commercially available and no custom designed optical components are used. The evaluation of several concepts for the design of the sending and receiving optics is shown in this chapter.

2.1 *System modeling*

A simulation model has been developed to assist the sensor system design.[16)] It is based on the Lidar Eq. (1) estimating the received signal power at the detector P_{det}. P_{L} is the sending beam power; β is the backscattering coefficient[19)] and ΔR is the scattering volume, together to describe the amount of light scattered back from the aerosols; $A/(4\pi R^2)$ is the amount of backscattering light to be collected; η_{coll}, η_{trans}, and η_{sys} are the efficiencies of collection, atmospheric transmission, and system loss; P_{B} is the back ground noise power.[20)]

$$P_{\mathrm{det}} = P_{\mathrm{L}} \cdot [\beta \cdot \Delta R] \cdot \left[\frac{A}{4\pi R^2}\eta_{\mathrm{coll}}\right] \cdot \eta_{\mathrm{trans}} \cdot \eta_{\mathrm{sys}} + P_{\mathrm{B}} \quad (1)$$

Within our earlier simulation using a 1 W laser transmitting to 100 m distance, with a receiver aperture diameter of 100 mm, depending on the contribution of aerosols, about 0.1–100 pW signal power can be collected by the receiver which is a very weak signal. However, this signal is passed to the coherent detection in order to be amplified to a detectable power. A reference beam with an electric field of $E_{\mathrm{ref}} = A_{\mathrm{ref}} e^{-jf_{\mathrm{ref}}t+\phi_{\mathrm{ref}}}$ is created to interfere with the scattered signal beam with an electrical field of $E_{\mathrm{s}} = A_{\mathrm{s}} e^{-jf_{\mathrm{s}}t+\phi_{\mathrm{s}}}$ to incident a total electric field $E_{\mathrm{out}} = A_{\mathrm{s}} e^{-jf_{\mathrm{s}}t+\phi_{\mathrm{s}}} + A_{\mathrm{ref}} e^{-jf_{\mathrm{ref}}t+\phi_{\mathrm{ref}}}$ on the detector. This is shown in Fig. 3. The optical power detected by a square law detector, e.g., a photo-diode, is proportional to the irradiance, which for the mixed fields is given as

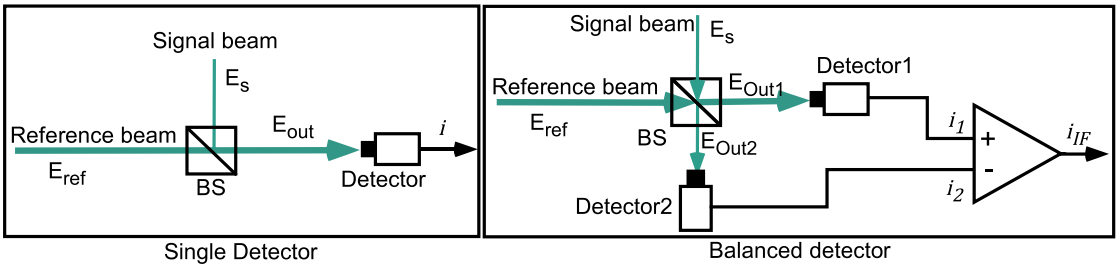

Fig. 3. (Color online) Coherent detection method to amplify the weak signal. Left: with single detector, right: with balanced detector configuration.

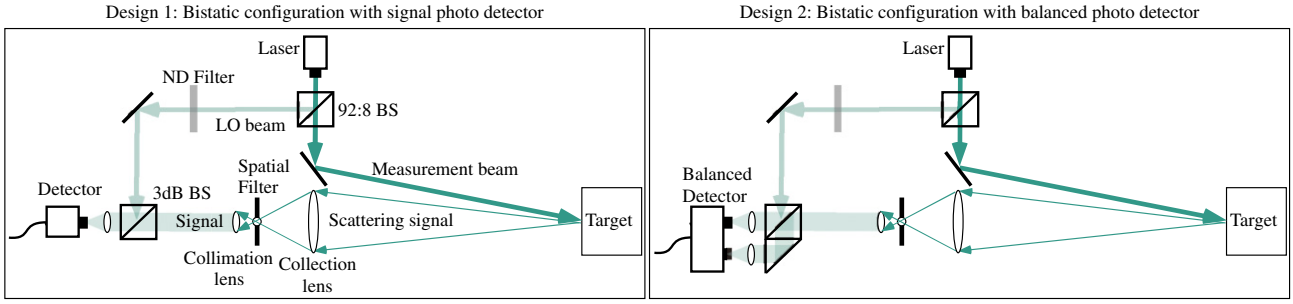

Fig. 4. (Color online) Free space bistatic configuration Doppler wind Lidar experimental setup with single photo detector (left) and balanced photo detector (right).

$$P_{\text{out}} = \frac{P_{\text{S}} + P_{\text{ref}}}{2} + \sqrt{P_{\text{S}} \cdot P_{\text{ref}}} \cdot \gamma(\Delta f) \cdot e^{-j(f_{\text{S}} - f_{\text{ref}})t + (\phi_{\text{S}} - \phi_{\text{ref}})}, \tag{2}$$

where $\gamma(\Delta f)$ is the coherent function of the laser with a Lorentzian spectrum bandwidth Δf.[21] Doppler frequency can be measured by analyzing the detector current. However, the strong DC power caused the excess noise which affects the detection strongly. A balanced detection configuration is proposed to reduce this noise (Fig. 3). The optical power at the detector can be evaluated with Eq. (3). In an ideal case, the DC part is completely subtracted:

$$P_{\text{out}} = \sqrt{P_{\text{S}} \cdot P_{\text{ref}}} \cdot \gamma(\Delta f) \cdot e^{-j(f_{\text{S}} - f_{\text{ref}})t + (\phi_{\text{S}} - \phi_{\text{ref}})}. \tag{3}$$

It is not possible to subtract all the DC component detectors by balanced detection due to the variance of the two detectors. The performance of a balanced detector is measured by the parameter "common-mode rejection ratio (CMRR)", which describes how much of the DC signal power will appear in the output [Eq. (4)], where V_{CM} is the common mode voltage (DC output) and V_{Bal} the AC carrier voltage which carries the beat frequency signal. Therefore, the optical power at the detector can be described with Eq. (5):

$$\text{CMRR (dB)} = 20 \cdot \log_{10}\left(\frac{V_{\text{CM}}}{V_{\text{Bal}}}\right), \tag{4}$$

$$P_{\text{out}} = \frac{P_{\text{S}} + P_{\text{ref}}}{2 \times 10^{\frac{\text{CMRR}}{20}}} + \sqrt{P_{\text{S}} \cdot P_{\text{ref}}} \cdot \gamma(\Delta f) \cdot e^{-j(f_{\text{S}} - f_{\text{ref}})t + (\phi_{\text{S}} - \phi_{\text{ref}})}. \tag{5}$$

2.2 *System design*

2.2.1 *(Design 1) Bistatic configuration with single photo detector*

In our previous work, an experimental setup (Fig. 4, left) was achieved that measured the speed of a solid spinning target or an aerosol seeded wind flow in a wind tunnel from 2 m distance (Fig. 5). A single longitudinal mode cw solid state laser with a wavelength of 532 nm and a coherence length of 50 m at 50 mW output power is used. The receiving optics is designed to collect the scattering light and collimate to a parallel beam. The reference beam is split by a 92:8 beam splitter (BS) and passes into the 50:50 BS to mix with the signal beam to create a coherent signal with a beat frequency, i.e., the Doppler shifted frequency. This signal is measured by the photo detector and is digitized for further analysis by a high speed digitizer (National Instruments PXI-5662) for the computer. The evaluation shows that the measurement distance is limited due to the high relative intensity noise (RIN) of the laser and the small reference beam power at the detector.

We substituted the single detector with a balanced detector in the second design to reduce the laser RIN noise from the strong reference beam by using the two output ports from the BS (Fig. 4, right). It turns out that the balanced detector concept reveals a SNR gain of 5 dB whereby the spinning target has been measured for both setups at the same speed (ca. 2.8 m/s, LOS) and distance (2 m) (Fig. 6). The higher absolute noise power from the balanced detector is due to the higher reference beam power. The advantages of the balanced detector concept are a better signal to noise ratio and a higher beam power with regards to the reference

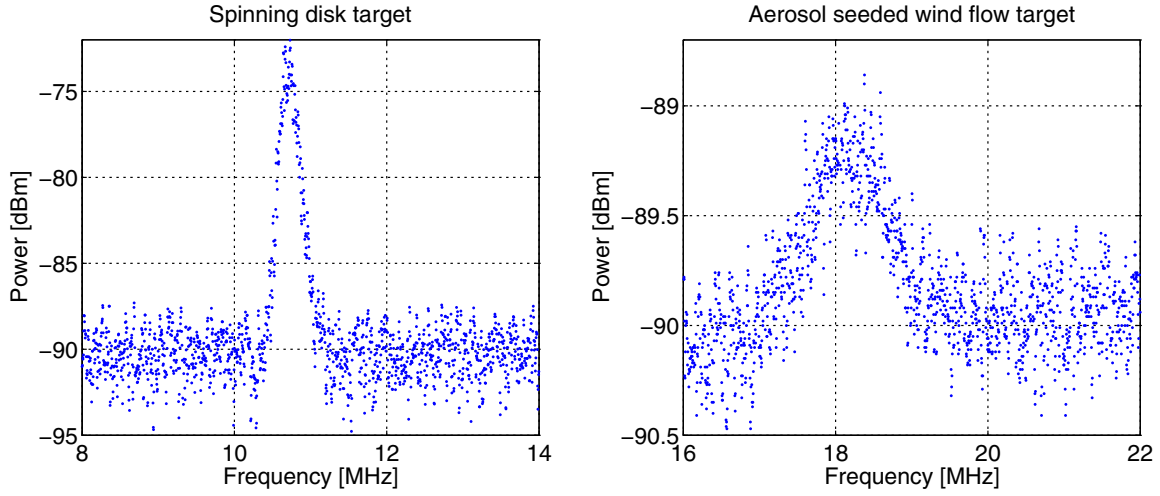

Fig. 5. (Color online) Experimental result with Design 1 (target distance 2 m). Left: from a spinning disk target. Right: from an aerosol seeded wind flow.

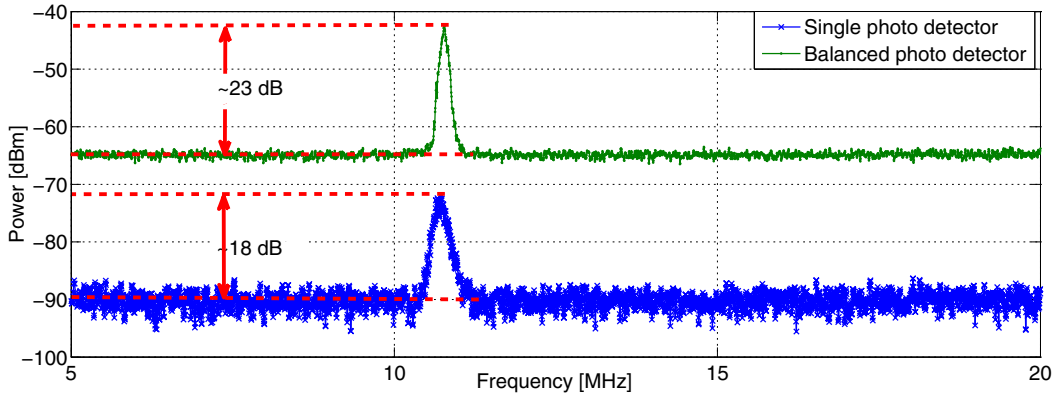

Fig. 6. (Color online) A comparison of experimental results from the setup with single (up) and balanced (down) detector (target distance 2 m).

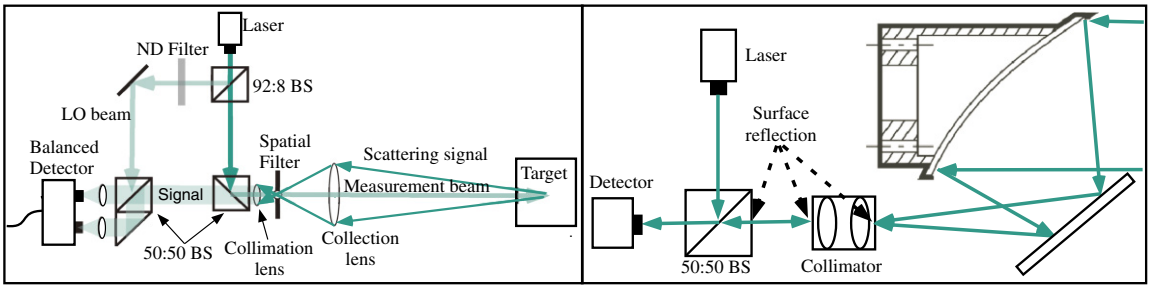

Fig. 7. (Color online) (Design 3) Left: Monostatic configuration with standard beam splitter. Right: Illustration of the beam circulator surface reflection.

beam. The flaw of this concept is that the readjustment of the bistatic free space setups can be very difficult.

2.2.2 *(Design 3) Monostatic configuration with standard beam splitter*

To overcome the realignment difficulties of the bistatic configuration, a monostatic configuration has been designed (Fig. 7) in which the transmitting and receiving optics share the same optical axis. Thus, a 50:50 BS has been added in Design 3 to redirect the measurement beam to the target in the former setups. The measurement beam and the back-scattering beam are on the same common optical axis in this configuration. But as a result of the additional surfaces of the optical components, a high noise is registered because each optical surface reflects 0.7% of the laser input power (Fig. 8). A coherent measurement could not been achieved.

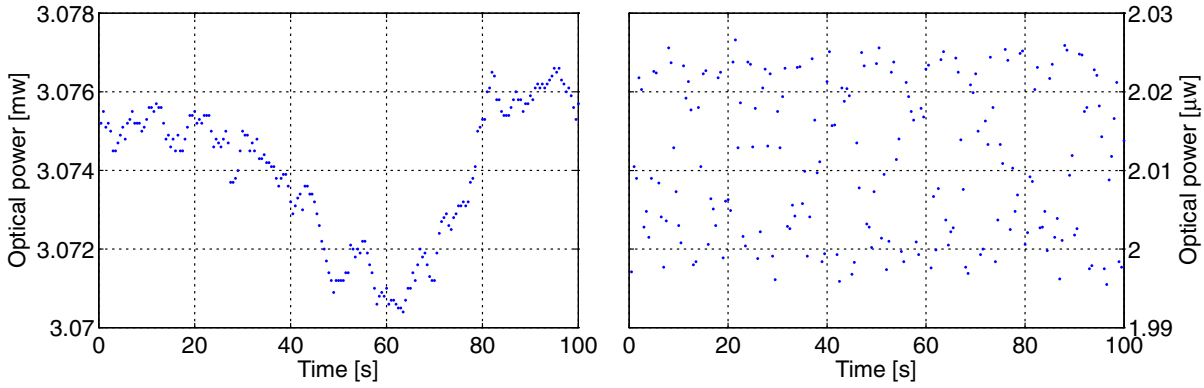

Fig. 8. (Color online) Measurement results of power transmitted to the collimator (left) and the reflection (right).

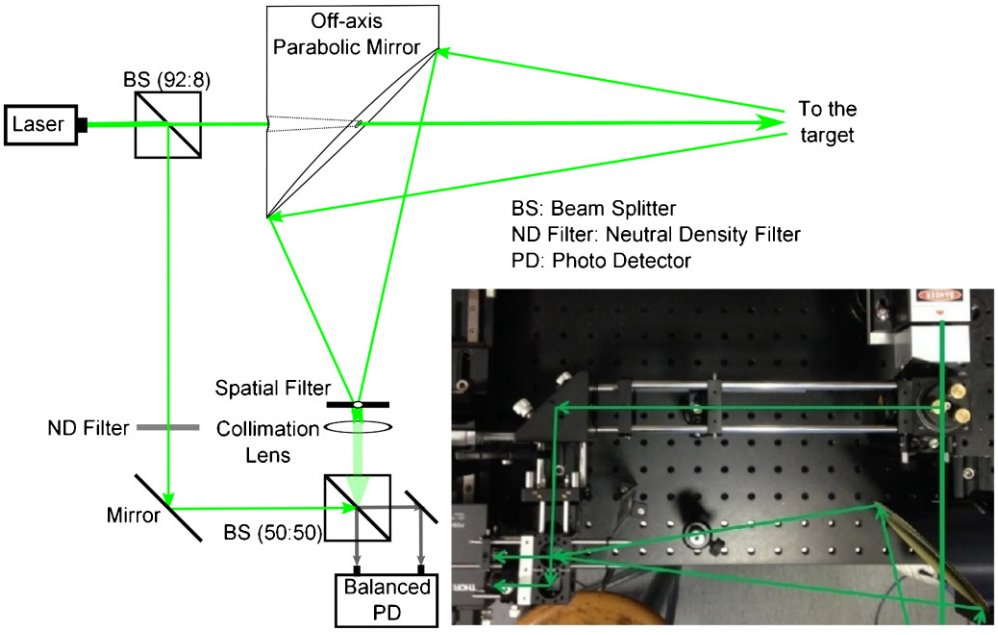

Fig. 9. (Color online) (Design 4) Monostatic configuration non-confocal system with off-axis parabolic mirror.

2.2.3 *(Design 4) Monostatic configuration non-confocal system with off-axis parabolic mirror*

In Design 4 an off-axis parabolic mirror with a center hole (Thorlabs MPD7621143-90-M01) substitutes the 50:50 BS (Fig. 9) to avoid the phase noise caused by additional surface reflections from the optical components. The sending beam passes through the center hole in the off-axis parabolic mirror and focused to the target distance. Since no interaction between the sending and receiving beam, the sending beam adds no direct noise to the detection. Figure 10 shows measurements on a spinner disk target for different measurement distances, and Fig. 11 shows the result from wind flow measurements. Assuming the reference power is stable, Eq. (3) shows the beat signal power, which depends on the signal power $P_S(d)$ and the coherence function $\gamma(d)$. Therefore, the beat signal amplitude can be describe with $f(d) = a \cdot d^{-1} \cdot e^{-b \cdot d}$, d is the distance. Assuming the noise floor is the same for different distance, then the SNR can be described as the same $\mathrm{SNR}(d) = a \cdot d^{-1} \cdot e^{-b \cdot d}$. We see the same trends from the experiment results. However, further experiments and analysis are required due to the high uncertainty and limited observability of noise.

3. Laser Safe Operation Consideration

To enable an easy access to the market, we were aiming for laser class 1 operation and assume pulse durations of 1–10 μs at a wavelength of 1550 nm for our system. The choice of the wavelength is based on the allowed emission power and the atmospheric transmission window in that region (Fig. 12). This leads to the following laser safety restrictions: The maximum permissible exposure (MPE) value is $1\,\mathrm{J/cm^2}$ which results in an accessible emission limit (AEL) of $8 \times 10^{-3}\,\mathrm{J}$ for class 1 operation.[23] For repetitive pulse sources the correction factor C_5 has to be multiplied with the emission limit for a single pulse (assume all pulses have the same pulse duration and are smaller 18 μs).[24] Hence:

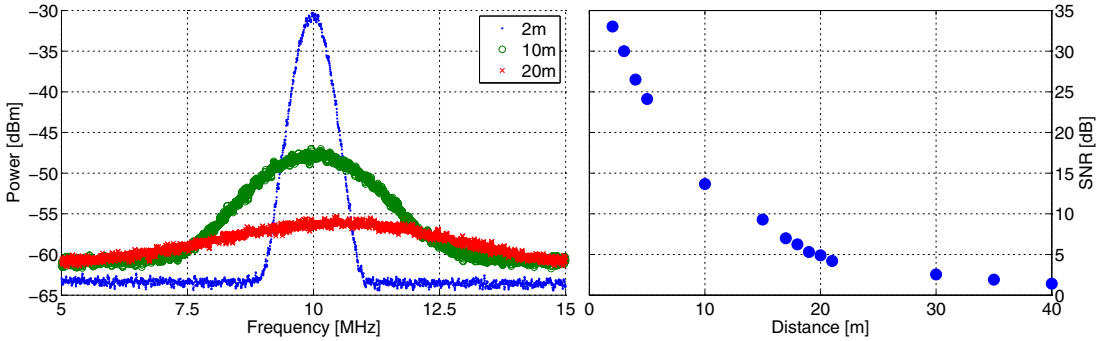

Fig. 10. (Color online) Left: Measurement result with Design 4 for different measurement distances. Right: SNR plot for different measurement distances.

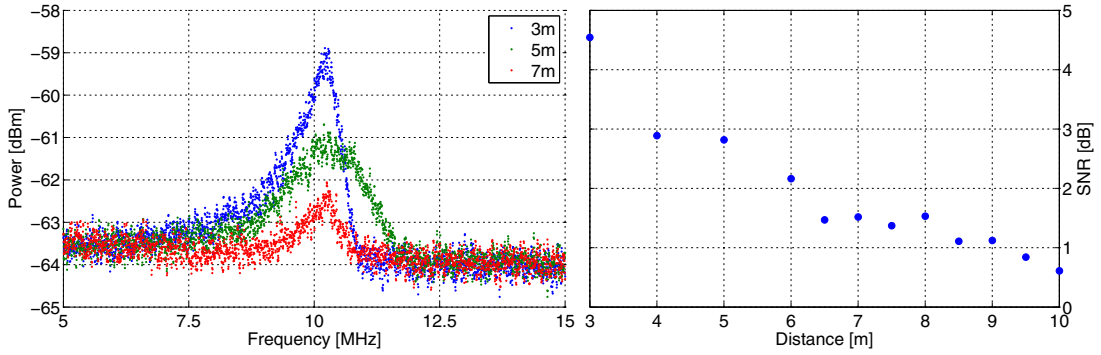

Fig. 11. (Color online) Left: Spectrum data with Design 4 for different measurement distances. Right: SNR plot for different measurement distances.

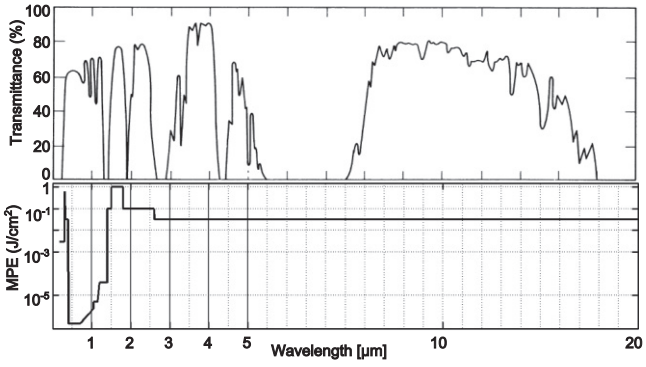

Fig. 12. Choice of the Lidar system wavelength, up) atmospheric transmittance,[22] down) *Maximum Permissible Exposure* (MPE) for eye safe operation.

$$\begin{aligned} \mathrm{AEL}_{\text{pulse train}} &= \mathrm{AEL}_{\text{single pulse}} \cdot C_5 \\ &= \mathrm{AEL}_{\text{single pulse}} \cdot N^{-0.25} \end{aligned} \tag{6}$$

with N being the number of pulses in the considered time frame, such as 10 s which leads to $N = 10000$ gives an allowed single pulse energy of 8×10^{-4} J. In the future, the suggested measurement technique might be combined with a laser scanning approach which would lead to different laser safety scenarios.[25,26] Additionally the revision of the laser safety standard might influence theses values.[27]

4. Conclusions

We documented details in this paper about the receiving and sending optics designs of a cost efficient coherent Doppler lidar system which was presented at the international conference on Optics–Photonics Design and Fabrication (ODF14) for assisting prediction based control of HAWT blade pitches. Four different optical receiving and sending system designs are discussed and evaluated via a free space coherent Doppler Lidar experimental setup with a spinner disk target and an aerosol seeded wind flow. Out of these four design concepts, the bi-static configuration shows the benefit of avoiding the noise from the strong sending beam, however, the alignment problems limit the application; the mono-static configuration with standard BS design shows a strong reflection on each optical component surface which leads to a high noise; the mono-static configuration non-confocal system design with a centered hole off-axis parabolic mirror overcomes those problems. Furthermore, other parts of the Lidar system design are going to be published in our upcoming publications.

Acknowledgments

We gratefully acknowledge the support for our research project "Laser-Doppler Windprofilmessung zur aktiven Lastregelung von Windkraftanlagen und zur Standortexploration (LAWAL), FKZ: 0325386A" by "BMWi (Federal Ministry for Economic Affairs and Energy)". We also thank the Karlsruhe School of Optics and Photonics (KSOP) for their support.

References

1) A. Scholbrock, P. Fleming, L. Fingersh, A. Wright, D. Schlipf, F. Haizmann, and F. Belen: Proc. 51st AIAA, 2013.
2) L. Y. Pao and K. E. Johnson: IEEE Control Systems **31** [2] (2011) 44.
3) L. Shinohara, T. Beuth, M. Fox, N. Heussner, H. Umesh-Babu, and W. Stork: Proc. ODF14, 2014.
4) L. Shinohara, S. Bogatscher, N. Heussner, H. Umesh-Babu, M. Brunet, and W. Stork: Proc. SPIE **8235** (2012) 823519.
5) R. M. Huffaker and R. M. Hardesty: Proc. IEEE **84** (1996) 181.
6) R. Frehlich, S. M. Hannon, and S. W. Henderson: J. Atmos. Oceanic Technol. **11** (1994) 1517.
7) N. Angelou, T. Mikkelsen, K. H. Hansen, M. Sjoeholm and M. Harris: Rep. RISO-R-1741(EN); TRN: DK1001124 (2010).
8) J. Vaughan and P. Forrester: Wind Eng. **13** [1] (1989).
9) D. A. Smith and M. Harris: US Patent 7281891 B2 (2007).
10) J. A. Zak and D. Rutishauser: Tech. Rep. NASA CR-212175 (2003).
11) C. Pedersen and R. Hansen: WO Patent 2009046717 (2009).
12) C. Pedersen, P. J. Rodrigo, and T. F. Q. Iversen: WO Patent 2013139347 (2013).
13) T. Burton, D. Sharpe, N. Jenkins, and E. Bossanyi: *Wind Energy Handbook* (Wiley, New York, 2001).
14) L. Shinohara, J. Asche-Tauscher, M. Fox, T. Beuth, and W. Stork: Proc. SPIE **9141** (2014) 91411M.
15) L. Shinohara, T. Beuth, M. Fox, and W. Stork: Proc. DGaO, 2014.
16) L. Shinohara, T. A. Pham Tran, T. Beuth, H. Umesh Babu, N. Heussner, S. Bogatscher, S. Danilova, and W. Stork: Proc. SPIE **8789** (2013) 87890V.
17) J.-P. Cariou: *Remote Sensing for Wind Energy* (DTU Wind Energy, 2013).
18) J.-P. Cariou, B. Augere, and M. Valla: C. R. Phys. **7** (2006) 213.
19) T. Beuth, L. Shinohara, M. Fox, and W. Stork: Proc. DGaO, 2014.
20) P. W. Milonni: *Lidar Range-Resolved Optical Remote Sensing of the Atmosphere* (Springer, Heidelberg, 2009).
21) J. W. Goodman: Goodman: *Statistical Optics* (Wiley, New York, 2000).
22) M. H. Frosz, M. Juhl, and M. H. Lang: *Optical Coherence Tomography: System Design and Noise Analysis* (Riso National Laboratory, 2001).
23) IEC 60825-1 (2007).
24) N. Heussner, S. Bogatscher, and W. Stork: to be published in J. Soc. Inf. Disp. (2014).
25) A. Frederiksen, R. Fiess, W. Stork, S. Bogatscher, and N. Heussner: J. BMTE **57** (2012) 175.
26) S. Bogatscher, C. Giesel, T. Beuth, H. Umesh-Babu, L. Shinohara, N. Heussner, A. Streck, and W. Stork: Proc. SPIE **8512** (2012) 85120E.
27) N. Heussner, S. Bogatscher, S. Danilova, and W. Stork: Proc. ODF14, 2014.